Adsorption of bentazon on two kinds of granular activated carbons: equilibrium, kinetic and thermodynamic studies

Xingya Wei[a], Naiyun Gao[a,*], Changjun Li[a], Jing Deng[b], Yanping Zhu[a], Qiongfang Wang[a]

[a]*State Key Laboratory of Pollution Control and Resource Reuse, Tongji University, 1239 SiPing Road, Shanghai 200092, China, email: weixingya369@163.com (X. Wei), Tel. +86 021 65982691; emails: gaonaiyun@126.com, gaonaiyun1@126.com (N. Gao), tj2007119@126.com (C. Li), zhuyanping0516@126.com (Y. Zhu), wqfang2010@126.com (Q. Wang)*
[b]*College of Civil Engineering and Architecture, Zhejiang University of Technology, Hangzhou 310014, China, email: seudjing@163.com*

ABSTRACT

The adsorption of bentazon on two types of granular activated carbons (GACs), VRU F36X16 (VRU) and WS-480 (WS) from aqueous solution was evaluated by kinetics, isotherms, and thermodynamic models in this study. The impacts of initial bentazon concentration, temperature, and initial solution pH were also investigated. The equilibrium adsorption capacity (q_e) of each GAC was appreciable under the experimental condition, especially VRU. For either GAC, the adsorption process fitted pseudo-second-order equation best and statistics matched two-step intra-particle diffusion model well. Dubinin–Radushkevich model was the most suitable one for bentazon adsorption on VRU, while Redlich and Peterson model best described bentazon adsorption on WS. Both for VRU and WS, the adsorption process was exothermic and belonged to physisorption. The q_e of VRU and WS increased as initial bentazon concentration increased, though the removal rate of bentazon decreased. 25℃ was the optimal condition for bentazon adsorption on either GAC, while the q_e of both GACs dropped as the temperature increased. Although the increase in pH could hinder bentazon adsorption on GACs significantly, there was a slight change in the adsorption capacities of VRU and WS when initial solution pH was in the range 5–9.

Keywords: Adsorption; Bentazon; Granular activated carbon; Kinetics; Isotherms; Thermodynamics

1. Introduction

Due to its easy-to-use and cost-effective solution to protect crops from insects and weeds, pesticides have been widely applied in agriculture all over the world. Herbicides, one of the biggest pesticide groups, are used mostly to prevent the growth of weeds. Because herbicides are effective and convenient, people use them in large scale, but such use engenders a further problem: most users are not aware of either the environmental or the health risks of the use/abuse of herbicides [1]. Herbicides are mostly toxic and some even carcinogenic to living systems, non-biodegradable and frequently detected in surface and ground waters [2]. The potential health hazards of these chemicals in

*Corresponding author.

drinking water have aroused more and more public attention in the past few years. Bentazon (3-(1-methylethyl)-1H-2,1,3-benzothiadiazin-4(3H)-one-2,2-dioxide) is a kind of post-emergence herbicide widely used for selective control of broadleaf weeds and sedges in beans, rice, corn, peanuts, and mint [3]. The main physical and chemical properties of bentazon are listed in Table 1. The half-life of bentazon is long and it cannot be degraded easily in nature. The oral and dermal absorption of bentazon are harmful and it can cause irritation to the eyes [4]. In drinking water, the maximum concentration of bentazon admitted by World Health Organization is 30 μg/L [5].

Because of the characteristics mentioned above, researchers have studied several methods to remove bentazon, such as photocatalytic degradation [6], adsorption [1,7,8] and advanced oxidation processes [9]. However, the studies mainly focused on the removal of bentazon in soil and only a few of investigations pay attention to the elimination of bentazon in aqueous solution with high concentration. Additionally, some of the adsorbents used in former experiments are not economical and the pre-processing steps are tedious, which make them not practical in water treatment. It is crucial to find a more appropriate way to solve these complications.

Granular activated carbon (GAC) is a kind of adsorbent that has the following advantages: large porous surface area, controllable pore structure, thermostability, and low acid/base reactivity [10]. It has the versatility for removal of a broad type of organic and inorganic pollutants dissolved in aqueous media [11,12], even from gaseous environment [13]. In this study, two kinds of common GACs, VRU F36X16 (VRU) and WS-480 (WS) were used to remove bentazon in aqueous solution.

The main objective of this research was to get the adsorption mechanism of bentazon onto GACs at low adsorbate concentration, which can play a guiding role in drinking water treatment when emergency deterioration of water quality occurs. The adsorption capacities of bentazon on VRU and WS were evaluated by

fitting data to different kinetic, isotherm and thermodynamic models. The effects of initial bentazon concentration, temperature, and initial solution pH on bentazon adsorption were assessed in this study as well.

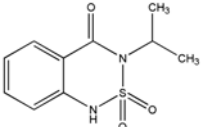## 2. Materials and methods

2.1. Chemicals

The adsorbate, bentazon used in the experiments was supplied by Sigma–Aldrich (St. Louis, MO, USA) and it was of analytical standard (Fluka) grade without further purification. The solvent, deionized water was obtained from a Millipore Milli-Q Academic Ultra Pure Water Purification System (TOC < 0.2 mg/L, resistivity > 18.2 MΩ) (Billerica, MA, USA). All other chemicals were at least analytical grade and obtained from Sinopharm Chemical Reagent Co., Ltd (Shanghai, China), except as otherwise noted.

2.2. Adsorbent preparation and characterization

The two kinds of GACs, VRU F36X16 (VRU) and WS-480 (WS) were obtained from Calgon Carbon (Tianjin) Co., Ltd. Both two GACs are coal-based activated carbons. Before batch adsorption experiments, the activated carbons were collected and washed with distilled water to remove the dirt, and then they were dried in the oven at 103°C for 24 h.

The surface morphologies of the two adsorbents were examined by a scanning electron microscope (SEM). The surface area and pore volume distributions of VRU and WS were measured by a Micromeritics ASAP 2020 surface area and porosity analyzer using a nitrogen adsorption–desorption method. The zeta-potential measurements were performed on a Malvern Zetasizer Nano ZS 90 immediately after the pH measurements of the pH titration samples. The applied adsorbents were also characterized by a Nicolet 5700 intelligent Fourier transformation infrared spectroscopy (FTIR).

Table 1
Important chemical/physical properties and chemical structure of bentazon

Pesticide	Formula	Chemical structure	Molecule weight (g/mol)	Solubility in water (g/L) (20°C)	Density (g/cm³)	Melting point (°C)
Bentazon	$C_{10}H_{12}N_2O_3S$		240.3	0.50	1.345	137–139

2.3. Adsorption experiments

The adsorption experiments of bentazon were performed in sealed 250-mL amber narrow mouth bottles. Each time 200 mL bentazon solution was added into the bottle. Batch adsorption experiments were performed on a shaker (HZQ-X300C constant temperature oscillator). The optimum dosages of VRU and WS, and the optimum speed of the temperature-controlled orbital shaker were obtained from the preliminary tests. Specifically, VRU and WS were added at the dosages of 0.010 and 0.046 g, respectively, and the experimental bottles were kept on the shaker for at least 4 d with the speed of 160 rpm in order to reach the adsorption equilibrium. The bentazon concentrations in solutions before and after adsorption were detected to compare the adsorption effects of two kinds of GACs. In the experiments, the initial bentazon concentrations were set in range 3, 4, 5, 6, and 7 mg/L to investigate its impact on adsorption. The adsorption experiments were performed at 15, 25, 35, 45, and 55°C separately to study the effect of temperature. Finally, bentazon solutions were adjusted by 0.1 M HCl or 0.1 M NaOH to make solution pH in the range 3, 5, 7, 9, and 11 to observe the influence of initial solution pH. The detected samples were collected in designated times each with a syringe and filtered through 0.22 μm filter for further analysis.

2.4. Analytical methods

The concentration of bentazon in solution was quantified using a reversed-phase high performance liquid chromatograph (HPLC) (Waters 2010, USA) with a – detector (Waters 2489) at the excitation wavelength of 225 nm, where bentazon had the maximum absorbance (see Supporting information, Fig. S1). The column used in HPLC was a reversed-phase Symmetry C18 column (250 mm × 4.6 mm i.d., 5 μm, Waters, USA). The injection volume of each sample was 10 μL and the column temperature was maintained at 40°C. The mobile-phase solvent profile was 20% Milli-Q ultrapure water and 80% methanol (Sigma–Aldrich) at a constant flow rate of 0.7 mL/min. The solution pH was monitored with a pH meter (FiveEasy™, Mettler-Toledo International Trading (Shanghai) Co., Ltd) equipped with pH electrode.

3. Results and discussion

3.1. Characterization

The SEM images for the surface morphologies of VRU and WS are included in Fig. 1. It indicates that compared to WS, the surface of VRU particles was more irregular containing more pores, which was more conducive to the adsorption of pollutants. Fig. 1 also shows the surface area and pore volume distributions of VRU and WS, and the main BET data are listed in Table 2. Particularly, the BET surface area is 678.71 and 732.16 m^2/g for VRU and WS, respectively. These high values reveal the existence of a high porosity responsible for the significant capacity of adsorption. For either GAC, the maximum incremental surface area and pore volume both came up at 2.16 nm pore width, implying that both GACs have abundant micropores to adsorb pollutants. However, the biggest difference between VRU and WS is that there almost no pore larger than 4.32 nm for WS while the pore width for VRU can even be larger than 25 nm. As a result, the BET pore volume and average pore size of VRU (0.42 cm^3/g, 2.47 nm) are larger than those of WS (0.38 cm^3/g, 2.09 nm). The pore volume distribution of VRU may be more conducive to the intra-particle diffusion which benefits the adsorption of bentazon.

Table 2 also shows the pH corresponding to point of zero charge (pH$_{PZC}$) which given by the curve of zeta-potential vs. pH (see Supporting information, Fig. S2). The pH$_{PZC}$ is around 3.19 and 2.94 for VRU and WS, respectively. This result indicates that both GACs may contain some acidic functional groups (phenol, carboxylic, carbonyl, etc.), which may play a positive role in the adsorption of bentazon. FTIR spectra of VRU and WS are shown in Fig. S3 (see Supporting information). The spectra of VRU show 3 bands which may correspond to C–O wag (at wavenumber of 1,090 cm^{-1}), aryl C–H wag (798 cm^{-1}), and aryl C–C wag (467 cm^{-1}), respectively, while the spectra of WS have no obvious bands at all. Specially, the presence of band attributed to the C–O stretching vibration in C–O–H at 1,090 cm^{-1} was reported to favor the adsorption of some pollutants [14]. Therefore, the –OH surface group seems to be an important factor for bentazon adsorption on VRU.

3.2. Effect of initial bentazon concentration

The effect of initial liquid-phase concentration of bentazon (C_0, mg/L) is shown in Fig. 2. The removal rate of bentazon was displayed by C/C_0. The adsorption capacity of bentazon on VRU or WS at a certain time t (h), q_t (mg/g), can be calculated by Eq. (1), while the equilibrium adsorption capacity, q_e (mg/g), can be calculated by Eq. (2):

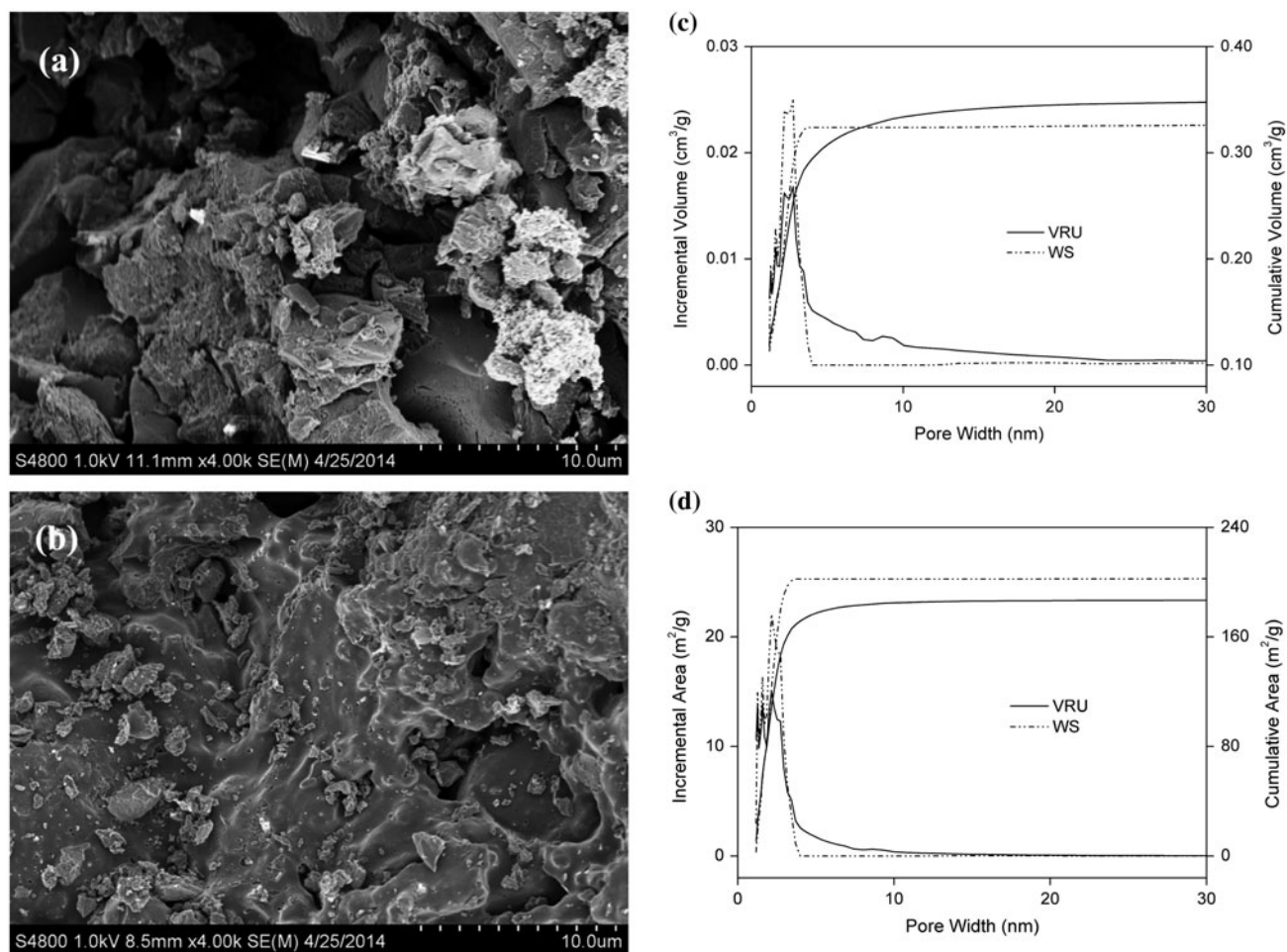$$q_t = \frac{(C_0 - C_t)V}{W} \tag{1}$$

Fig. 1. Left: SEM images for the surface morphology of VRU (a) and WS (b). Right: pore volume (c) and surface area (d) distributions of VRU and WS.

Table 2
Some chemical/physical characterization results of VRU and WS

GACs	BET surface area (m²/g)	BET pore volume (cm³/g)	Average pore size (by BET) (nm)	pH$_{PZC}$
VRU	678.71	0.42	2.47	3.19
WS	732.16	0.38	2.09	2.94

$$q_e = \frac{(C_0 - C_e)V}{W} \qquad (2)$$

where C_t (mg/L) is the liquid-phase concentration of bentazon at the certain time t, C_e (mg/L) is the equilibrium concentration of bentazon in solution, V (L) is the solution volume, and W (g) is the weight of adsorbent used in the experiment.

Overall, the adsorption capacities of both GACs increased along with the increase in C_0. Particularly, as C_0 increased from 3 to 7 mg/L, the q_e of VRU and WS increased from 45.6 and 11.9 mg/g to 87.0 and 24.5 mg/g, respectively. This could be attributed to the higher concentration gradient existing in the higher concentration solution which acts as a driving force for the adsorption process [15]. Even so, the removal rate of bentazon decreased when C_0 increased from 3 to 7 mg/L both for VRU (from 75.9 to 62.1%) and WS (from 91.0 to 80.4%). This is probably because C_0 increased faster than q_e of GACs. Although the eventual removal rate of bentazon for WS was slightly higher than that for VRU, the q_e of VRU was much
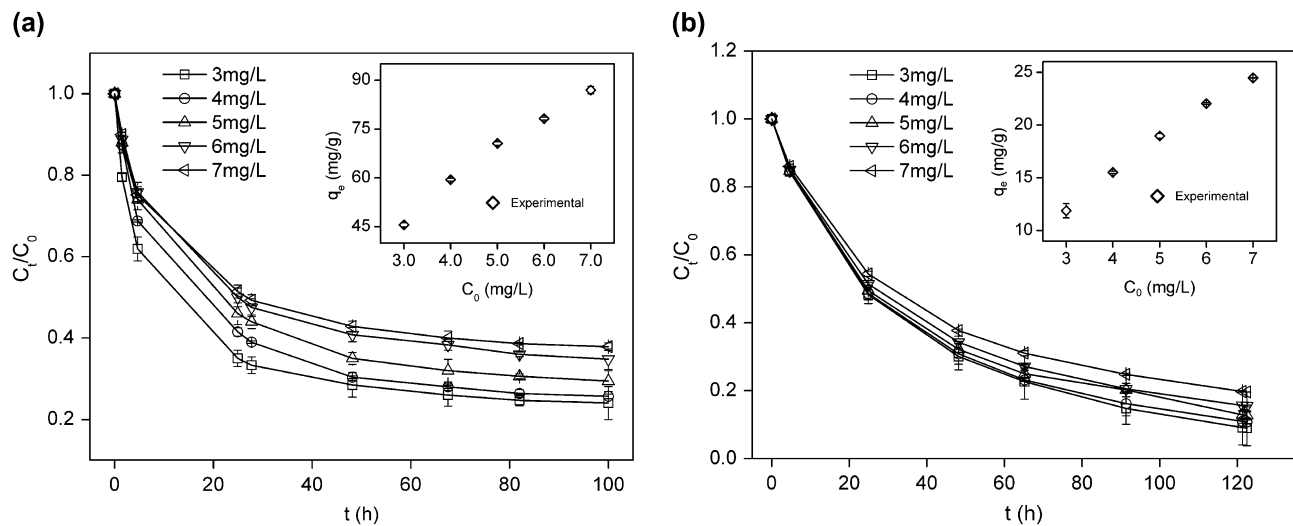
(a)

(b)

Fig. 2. Removal efficiency for bentazon adsorption onto VRU (a) and WS (b) at different C_0 (inset: plots of q_e vs. C_0). Experimental conditions: 25°C; pH not adjusted; agitation speed, 160 rpm; VRU dose, 50 mg/L; WS dose, 230 mg/L.

higher than q_e of WS. What is more, the q_e of WS always accounted for only a quarter of VRU's q_e, no matter what C_0 was. The differences in adsorption capacities can be associated with the properties of adsorbents. As mentioned in characterization, the presence of bigger pore and −OH surface group can be conducive to the adsorption of bentazon on VRU, leading to the higher q_e. Besides, the rules between the q_e of GACs (or removal rate of bentazon) and C_0 that mentioned above can apply to 15 and 35°C as well (see Supporting information, Figs. S4 and S5).

In addition, as listed in Table 3, at higher concentration of bentazon (25–200 mg/L), the q_e of VRU and WS were evaluated (see Supporting information, Fig. S6) and compared with various adsorbents reported in the literature for the adsorptive removal of bentazon. The maximum adsorption capacities of VRU and WS were 403.76 and 318.72 mg/g, respectively, which were much higher than those adsorbents used in previous work as reported (no more than 174.82 mg/g) [7,8,15–17]. The results demonstrated that both two kinds of GACs used in the study had obvious and considerable efficiency for the removal of bentazon in solution, especially VRU.

3.3. Adsorption kinetics

To study the adsorption mechanism which controls the adsorption process, the experimental data were fitted to four kinetic models including the pseudo-first-order (PFO), the pseudo-second-order (PSO), the Elovich, and the intra-particle diffusion models.

The PFO kinetic model can be expressed as Eq. (3) [18]:

$$q_t = q_e(1 - e^{-k_1 t}) \tag{3}$$

where k_1 (1/h) is the rate constant of the pseudo-first-order adsorption.

The PSO kinetic equation is given by Eq. (4) [19]:

$$q_t = \frac{q_e^2 k_2 t}{1 + q_e k_2 t} \tag{4}$$

where k_2 (g/(mg h)) is the pseudo-second-order rate constant.

The Elovich kinetic equation is written as Eq. (5):

$$q_t = a + b \log t \tag{5}$$

where a and b are Elovich rate constants.

The intra-particle diffusion equation has the form as Eq. (6):

$$q_t = k_{int} t^{1/2} + C \tag{6}$$

where k_{int} (mg/(g h$^{1/2}$)) is the intra-particle diffusion rate constant and C is the intercept, which represents the thickness of the boundary layer.

PSO model agrees with that adsorption is not just based on rapid adsorption but on complex processes including intra-particle diffusion and so on, while

Table 3
Comparison of equilibrium adsorption capacities of VRU and WS for bentazon with other adsorbents

Pesticide	Adsorbent	pH	Temperature (℃)	Pesticide initial concentration (mg/L)	q_m (mg/g)	Refs.
Bentazon	AC cloth	5.5	rt	50–200	115	[16]
	Oxidized AC cloth	5.5	rt	50–200	17	[16]
	Garden waste compost	7.7	rt	1–250	54.67	[17]
	Sandy loam soil	6.9	rt	1–250	6.67	[17]
	Date seed activated carbon	5.5	30	25–250	82.26	[15]
	Sky fruit husk activated	5.0	30	25–250	166.67	[8]
	Mesoporous phenolic resin	2.0	25	25–250	129.20	[7]
	Mesoporous carbon	4.0	25	25–250	174.82	[7]
	VRU	5.0	25	25–200	403.76	This study
	WS	5.0	25	25–200	318.72	This study

PFO model considers the rapid adsorption as major factor and is mainly monolayer adsorption. Elovich model describes a mix adsorption mechanism of rapid and slow adsorption. As shown in Table S1 (see Supporting information), the adsorption capacities of GACs had a greater relationship with pore volume rather than surface area of GACs, which implied that the adsorption of bentazon on GACs was not simple monolayer adsorption and tended to fit PSO model rather than PFO model. The fitted kinetics plots for bentazon adsorption on VRU and WS at 25℃ are shown in Fig. 3, and parameters including k_1, k_2, a, b, k_{int}, C and correlation coefficients (R^2) are listed in Table 4. The fitted result demonstrated that although there were big differences between the values of q_e on VRU and WS, PSO model was the most suitable one for bentazon adsorption on either kind of GAC among PFO, PSO, and Elovich models, and Salman et al. [15] also gave the same result. Moreover, the Elovich model also fitted the data better than PFO model. These all were because of the existence of intra-particle diffusion, which was confirmed by Fig. 5(b) and (d) as q_t vs. $t^{1/2}$ was well linear. For either of GACs, the adsorption process can be divided into two steps. In the first step, the lines were sharp and external surfacing adsorption was the key process. In the second step, the slopes of lines became smaller than those in the first step, which mainly because of the rate-controlling of intra-particle diffusion. However, the lines on either step did not pass through the origin, which demonstrated that the rate-limiting was not only due to the intra-particle diffusion. In addition, the experiments at 15 and 35℃ could further demonstrate the goodness-of-fit to PSO model and the rate-controlling of intra-particle diffusion (see Supporting information, Figs. S7 and S8, Tables S2 and S3).

3.4. Adsorption isotherms

In order to obtain the best fitting isotherm, five common isotherm models, Langmuir, Freundlich, Redlich and Peterson (RP), Temkin, and Dubinin–Radushkevich (DR) isotherm models were applied to fit the equilibrium data at 25℃.

The Langmuir isotherm model is given by Eq. (7) [20]:

$$q_e = \frac{q_m K_L C_e}{1 + K_L C_e} \tag{7}$$

where q_m (mg/g) is the maximum adsorption capacity, and K_L (L/mg) is the equilibrium adsorption constant which is related to adsorption energy.

The Freundlich isotherm model is written by Eq. (8) [21]:

$$q_e = K_F C_e^{1/n} \tag{8}$$

where K_F ((mg/g) (L/mg)$^{1/n}$) is the adsorption coefficient, which related to the adsorption capacity of adsorbents; n is a measure of the adsorption intensity and gives indication on the favorability of the adsorption.

The RP isotherm model can be expressed as Eq. (9) [22]:

$$q_e = \frac{K_{RP} C_e}{1 + \alpha_{RP} C_e^{\beta_{RP}}} \tag{9}$$

K_{RP} is the RP model isotherm constant (L/g), α_{RP} is the RP model constant (L/mg), and β_{RP} is the RP model exponent.
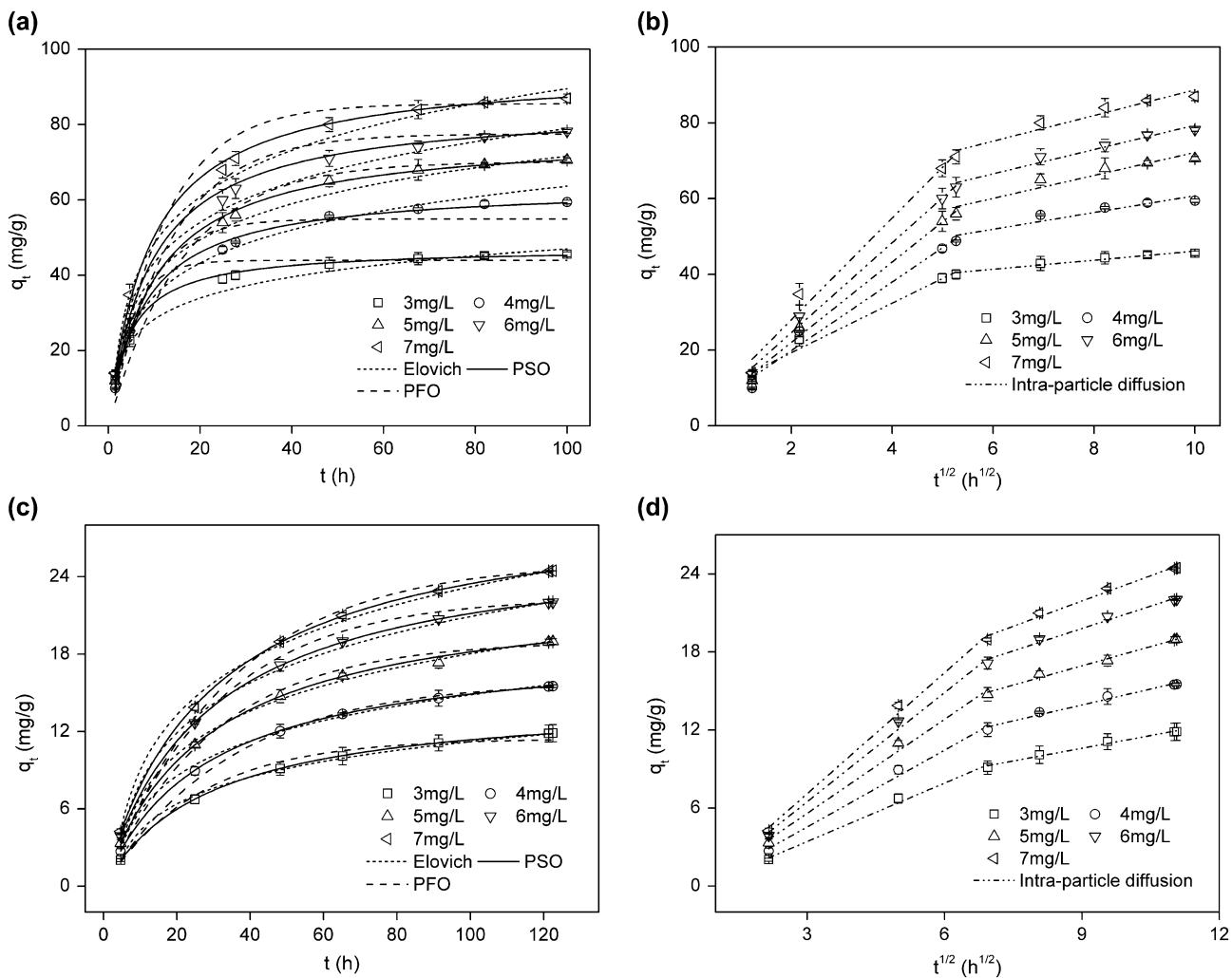
(a)

(b)

(c)

(d)

Fig. 3. Kinetics modeling for bentazon adsorption onto VRU (a and b) and WS (c and d). Experimental conditions: 25°C; pH not adjusted; agitation speed, 160 rpm; VRU dose, 50 mg/L; WS dose, 230 mg/L.

The equation of Temkin isotherm model can be written as Eq. (10):

$$q_e = \frac{RT}{b} \ln(K_T C_e) \qquad (10)$$

where b (kJ/mol) is the Temkin constant related to the heat of adsorption, K_T (L/g) is the Temkin isotherm constant, R (8.314×10^{-3} kJ/(K mol)) is the gas constant, and T (K) is the absolute temperature.

The DR equation has the form as Eq. (11) [23]:

$$\ln q_m = \ln q_m - B_{DR}\varepsilon^2 \qquad (11)$$

where ε is the Polanyi potential and B_{DR} (mol²/kJ) is the Dubinin–Radushkevich isotherm constant. The relationship among ε, T, C_e is given by Eq. (12):

$$\varepsilon = RT \ln(1 + 1/C_e) \qquad (12)$$

The fitted adsorption isotherms of bentazon on VRU and WS are shown in Fig. 4, and all related parameters are listed in Table 5. Comparing the correlation coefficients (R^2) of all isotherm models, the DR and RP isotherm models were found to fit the adsorption data of bentazon on both GACs better than other isotherm models, and they had almost the same goodness-of-fit. Particularly, the DR isotherm model fitted the adsorption data of bentazon on VRU best, while RP isotherm model could best describe the adsorption of bentazon on WS.

DR isotherm is an empirical model that following a pore-filling mechanism [24]. It is generally applied to express the adsorption mechanism with a Gaussian

Table 4
Pseudo-first-order, pseudo-second-order, Elovich and intra-particle diffusion model rate constants for adsorption of bentazon onto VRU and WS at 25°C

C_0 (mg/L)	Pseudo-first-order			Pseudo-second-order		
	$q_{e,cal}$ (mg/L)	k_1 (1/h)	R^2	$q_{e,cal}$ (mg/L)	$k_2 \times 10^3$ (g/(mg h))	R^2
VRU						
3	43.950	0.200	0.977	47.307	4.743	0.998
4	54.930	0.123	0.981	63.765	2.041	0.998
5	70.135	0.062	0.973	77.619	1.304	0.998
6	77.498	0.075	0.982	85.104	1.307	0.999
7	85.509	0.083	0.989	94.961	1.190	0.999
WS						
3	11.446	0.038	0.993	14.662	2.340	0.999
4	15.911	0.029	0.993	19.045	1.887	0.999
5	19.019	0.033	0.992	23.231	1.545	0.999
6	22.391	0.033	0.997	27.099	1.311	0.999
7	25.151	0.029	0.994	30.221	1.147	0.999

| Elovich			Intra-particle diffusion					
a	b	R^2	k_{int1} (mg/(g h$^{1/2}$))	C_{int1}	R^2	k_{int2} (mg/(g h$^{1/2}$))	C_{int2}	R^2
VRU								
9.577	18.714	0.987	6.544	6.216	0.971	1.195	34.176	0.940
5.293	29.176	0.995	9.065	1.724	0.968	2.215	38.603	0.865
8.083	31.767	0.981	10.623	0.762	0.990	3.027	41.894	0.885
7.742	35.589	0.995	11.886	0.818	0.985	3.205	47.296	0.953
7.358	41.082	0.996	13.439	1.109	0.977	3.388	54.818	0.916
WS								
-2.607	6.911	0.999	1.497	-1.067	0.987	0.652	4.722	0.986
-3.151	8.999	0.996	1.969	-1.362	0.985	0.817	6.572	0.979
-4.312	11.171	0.997	2.410	-1.634	0.992	0.987	8.048	0.987
-4.915	12.917	0.999	2.797	-1.904	0.987	1.147	9.473	0.979
-5.170	14.194	0.998	3.099	-2.195	0.990	1.295	10.258	0.985
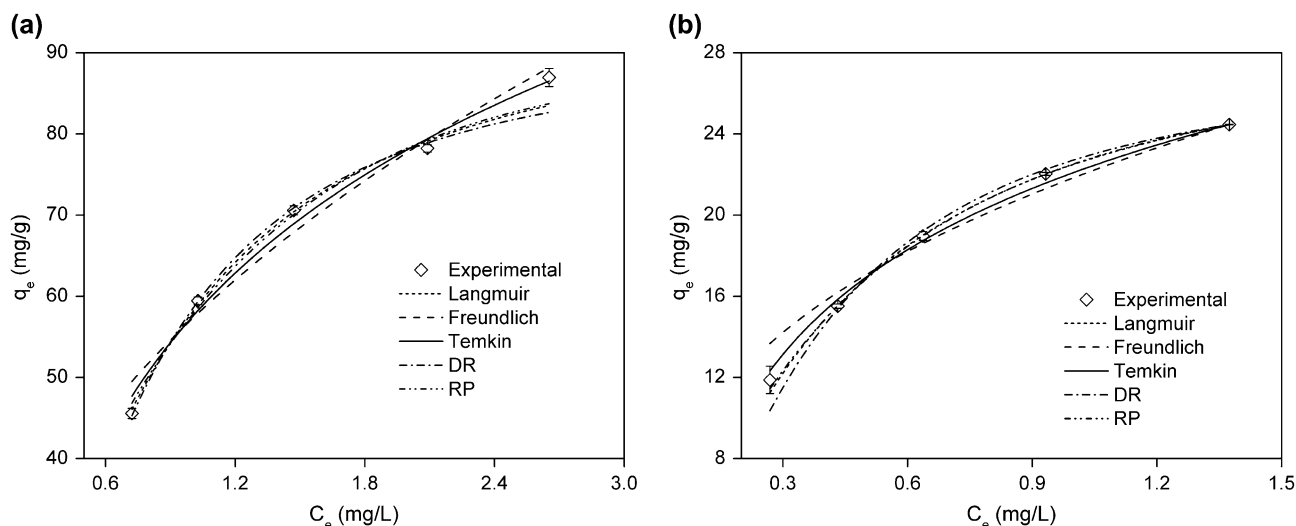
Fig. 4. Adsorption isotherms fitting for bentazon adsorption onto VRU (a) and WS (b). Experimental conditions: 25°C; pH not adjusted; agitation speed, 160 rpm; VRU dose, 50 mg/L; WS dose, 230 mg/L.

energy distribution onto a heterogeneous surface [25]. One of the unique features of the DR isotherm model lies on the fact that it is temperature-dependent. The adsorption data of bentazon on GACs matching the DR curve well indicated that the adsorption process had a great relationship with temperature. Moreover, unlike WS, the adsorption on VRU matching the DR curve best among isotherms models implied that it was more temperature-dependent than adsorption on WS, which will be demonstrated later.

RP isotherm is a hybrid isotherm featuring both Langmuir and Freundlich isotherms. Langmuir isotherm is more suitable for homogeneous surface adsorption and monolayer coverage at high concentration [26,27], while Freundlich isotherm fits heterogeneous surface and multilayer adsorption better at low concentration [11]. Therefore, RP isotherm can be applied both in homogeneous and heterogeneous systems due to its versatility [28]. The adsorption data of bentazon on either GAC fitting the RP curve well indicated that each adsorption process was not just simple monolayer adsorption but a complex process including intra-particle diffusion and so on. Moreover, the adsorption on WS matching the DR curve better than adsorption on VRU implied that the intra-particle diffusion played a more important role in the adsorption process of bentazon on WS, which can be confirmed in kinetics data (Table 4).

Additionally, the adsorption of bentazon on VRU and WS at 15 and 35°C could also fit DR and RP isotherm models well (see Supporting information, Figs. S9 and S10, Tables S4 and S5). This further demonstrated that the bentazon adsorption on

GACs had strong relationship with experiment temperature, which will be discussed later in adsorption thermodynamic.

3.5. Effect of temperature

As shown in Fig. 5, temperature had great influence on bentazon adsorption on VRU or WS. In the experiments, it was noted that 25°C was the optimal temperature condition for both kinds of GACs, and 15°C was the suboptimal condition. From 25°C, the adsorption capacities of GACs fell down with the increase in temperature. This phenomenon can be explained in two aspects as follows. On one hand, elevating temperatures resulted in strengthening the mobility of bentazon molecules from the solution towards the GAC surface and enhancing the rate of intra-particle diffusion [29], which benefited the adsorption. On the other hand, the opposite trend that adsorption capacities decreased as temperature increased from 25 to 55°C could be interpreted by the increase in bentazon solubility and the enhancing oscillation energy of bentazon molecules, which led to the decrease in adsorption force and more desorption from surface phase to liquid phase [2].

As mentioned before, no matter what C_0 was, the percent that q_e of WS accounting for q_e of VRU remained stable under the same temperature. Moreover, when temperature increased from 15 to 55°C, the q_e of WS narrowed the gap with that of VRU from 73 to 70%. This was probably due to the fact that bentazon adsorption on VRU was more temperature-dependent than the adsorption on WS, which has been

Table 5
Langmuir, Freundlich, RP, Temkin, and DR isotherm model parameters and correlation coefficients for adsorption of bentazon onto VRU and WS at 25°C

	Langmuir			Freundlich			RP				Temkin			DR		
	K_L (L/mg)	q_m (mg/g)	R^2	K_F ((mg/g)(L/mg)$^{1/n}$)	n	R^2	K_{RP} (L/g)	α_{RP} (L/mg)	β_{RP}	R^2	K_T (L/g)	b (kJ/mol)	R^2	B_{DR} (mol^2/kJ^2)	q_m (mg/g)	R^2
VRU	0.900	121.483	0.982	57.207	2.255	0.955	84.975	0.473	1.306	0.988	6.854	0.083	0.981	0.150	90.812	0.990
WS	2.122	32.855	0.990	21.846	2.804	0.978	57.017	1.531	1.144	0.999	19.466	0.333	0.986	0.066	27.629	0.998

discussed in isotherms and will be demonstrated in thermodynamic.

3.6. Adsorption thermodynamic

The differences in adsorption capacities are associated with the properties of adsorbents, such as structure, functional groups, pH$_{PZC}$, surface area, and so on. Most studies only investigated the adsorption capacity of an adsorbent and few simultaneously determined the adsorption capacity and related thermodynamics parameters [30]. The thermodynamic parameters, Gibb's free energy change ($\Delta G°$, kJ/mol), enthalpy change ($\Delta H°$, kJ/mol), and entropy change ($\Delta S°$, kJ/(mol K)) are calculated by Eqs. (13) and (14):

$$\Delta G° = -RT \ln K_{ad} \tag{13}$$

$$\Delta G° = \Delta H° - T\Delta S° \tag{14}$$

Combining equations above it can be concluded:

$$\ln K_{ad} = \frac{-\Delta G°}{RT} = \frac{\Delta S°}{R} - \frac{\Delta H°}{RT} \tag{15}$$

where K_{ad} is the adsorption equilibrium constant of the thermodynamic model. In this experiment, the adsorption equilibrium constants were achieved by the following method: as the concentrations of bentazon decreased and approached to 0, values of K_{ad} were obtained by plotting straight lines of (q_e/C_e) vs. q_e based on a least-square analysis and when extrapolating q_e to 0, the intercepts of vertical axis gave the K_{ad} values. The $\Delta H°$ and $\Delta S°$ were determined from the slope and intercept of the Van't Hoff plots of $\ln K_{ad}$ vs. $1/T$, respectively, and the $\Delta G°$ was determined from Eq. (13).

Table 6 summarizes the values of thermodynamic parameters mentioned above, which shows that $\Delta H°$, $\Delta S°$, and $\Delta G°$ were negative in the adsorption process of bentazon both on VRU and WS. The $\Delta G°$ values were negative at all experimental temperatures (15–55°C), which verified that the adsorption of bentazon onto GAC was spontaneous and thermodynamically favorable. Generally, more negative $\Delta G°$ implies larger driving force of adsorption, resulting in greater adsorption capacity. However, as temperature increased from 15 to 55°C, the $\Delta G°$ value turned to less negative, which indicated that the spontaneous nature of adsorption was directly proportional to the temperature. What is more, during the increase in temperature, the change in $\Delta G°$ value for adsorption on VRU was greater than that for adsorption on WS, which
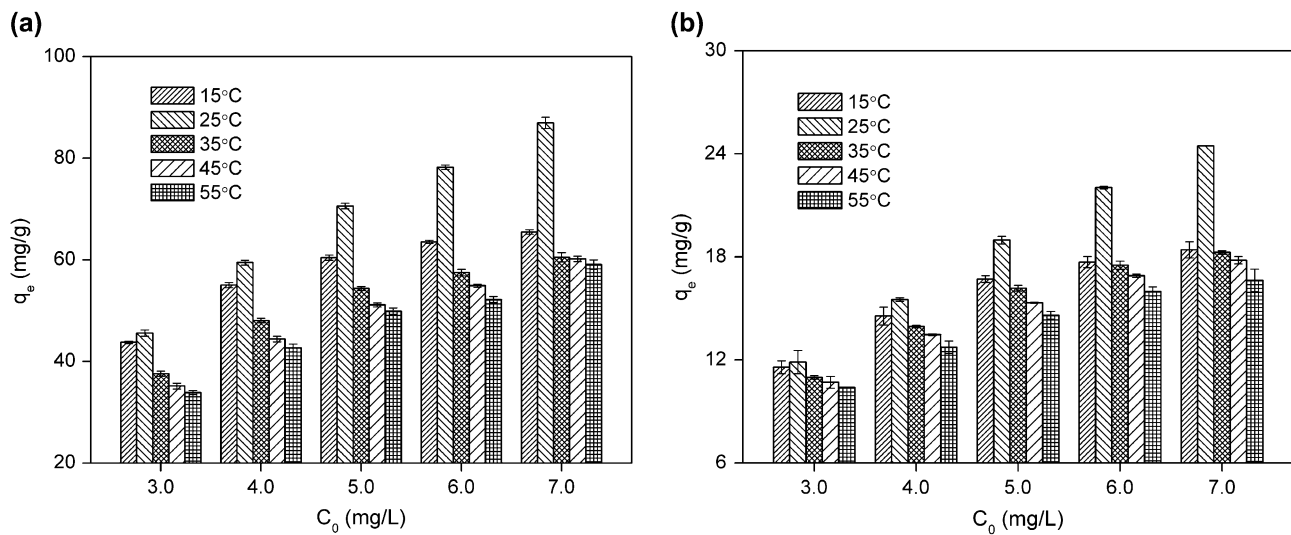
(a)

(b)

Fig. 5. Temperature effect on bentazon adsorption onto VRU (a) and WS (b). Experimental conditions: pH not adjusted; agitation speed, 160 rpm; VRU dose, 50 mg/L; WS dose, 230 mg/L.

demonstrated that bentazon adsorption on VRU was a more temperature-dependent process. The negative $\Delta H°$ value demonstrated that bentazon adsorption in experiment was an exothermic process, which is also supported by the decrease in q_e when temperature increased from 25 to 55°C. The negative $\Delta S°$ suggests that the degrees of freedom at the solid–liquid interface decreased during the adsorption.

Physisorption and chemisorption can be classified, to a certain extent, by the magnitude of $\Delta G°$ and $\Delta H°$. The numerical value of $\Delta G°$ for physisorption is less than that for chemisorption, the former between −20 and 0 kJ/mol while the latter between −400 and −80 kJ/mol [31]. As for $\Delta H°$, the physisorption bond strengths are typically considered to be less than 84 kJ/mol, while chemisorption ones can be 84–420 kJ/mol [32]. As shown in Table 6, the values of $\Delta G°$ for adsorption on both GACs were all between −9 and −12 kJ/mol, and the $\Delta H°$ was −23.449 and −17.088 kJ/mol for adsorption on VRU and WS, respectively, which all indicated that the adsorption of bentazon on VRU or WS was a physisorption process. As mentioned before, the –OH surface group on VRU seems to play a positive role on bentazon adsorption. Besides, after the equilibrium adsorption of bentazon ($C_0 = 200$ mg/L), the FTIR spectra of VRU indicated that the peak corresponding to the C–O stretching vibration in C–O–H at 1,090 cm^{-1} disappeared (see

Table 6
Thermodynamic parameters of bentazon adsorption on VRU and WS under different temperatures

T (K)	ln K_{ad}	$\Delta G°$ (kJ/mol)	$\Delta H°$ (kJ/mol)	$\Delta S°$ (kJ/(mol K))
VRU				
288.15	4.868	−11.663	−23.449	−0.041
298.15	4.618	−11.447	−23.449	−0.041
308.15	4.186	−10.725	−23.449	−0.041
318.15	3.883	−10.271	−23.449	−0.041
328.15	3.749	−10.228	−23.449	−0.041
WS				
288.15	4.398	−10.536	−17.088	−0.023
298.15	4.224	−10.471	−17.088	−0.023
308.15	3.880	−9.941	−17.088	−0.023
318.15	3.709	−9.810	−17.088	−0.023
328.15	3.572	−9.745	−17.088	−0.023

Supporting information, Figs. S3 and S11). Therefore, the adsorption on VRU may include some part of chemisorption, leading to the higher value of $\Delta H°$. On the other hand, the comparison of FTIR spectra of WS before and after adsorption demonstrated that either adsorption process in experiments belonged to physisorption.

3.7. Effect of initial solution pH

The interaction between the adsorbates and adsorbents can be influenced by pH; as a result, the amount of bentazon adsorption on GACs will alter with the changing solution pH. The effect of initial solution pH (pH_0) on the adsorption of bentazon on VRU and WS is shown in Fig. 6.

Fig. 6 indicates that for either GAC, the increase in pH_0 led to the decrease in adsorption capacity. Particularly, both for VRU and WS, the q_e at pH_0 3 (91.87 and 19.10 mg/g) was clearly larger than those at pH_0 11 (18.94 and 13.57 mg/g), meaning that changes in pH affected the adsorption capacities of GACs obviously. For either VRU or WS, the adsorption process and q_e were very close when pH_0 was 5, 7 and 9, indicating that the adsorption capacity of both GACs could keep stable in most of the actual water in nature and waterworks. This was because all these solution pH changed to near 6 soon after the start of adsorption (see Fig. 6(b) and (d)). Compared to the solution without bentazon, the change in solution pH during the process was mainly ascribed to the performance of GACs (see Supporting information,
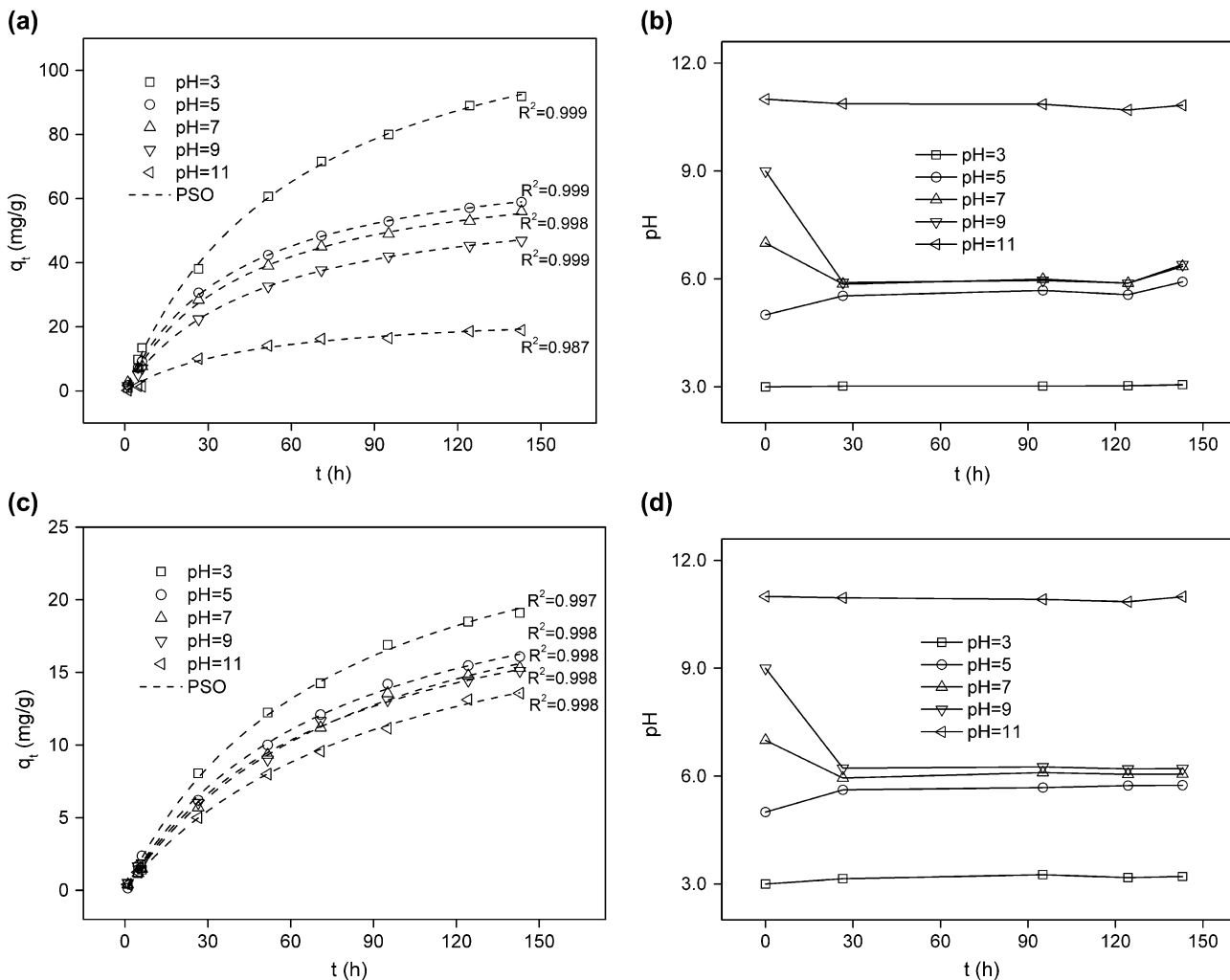

Fig. 6. Effect of initial solution pH on bentazon adsorption onto VRU (a) and WS (c) (fitting PSO kinetics), and pH change during adsorption processes of VRU (b) and WS (d). Experimental conditions: 25℃; without buffer solution; agitation speed, 160 rpm; C_0, 5 mg/L; VRU dose, 50 mg/L; WS dose, 230 mg/L.

Table S6). Moreover, to some extent, the q_e of VRU or WS was still decreased as pH_0 increased from 5 to 9.

The GAC surface and the adsorbate species coexisted in a complex system at a certain pH. The effect of solution pH on bentazon adsorption seemed to relate to both the change in bentazon existing form and the changes in GAC structure. Firstly, bentazon is a kind of weak acid with pK_a of 3.3 (25°C) and pH could change the existing formation of bentazon molecule in aqueous solution [16] (see Supporting information, Fig. S12). Most of bentazon was neutral molecule when pH < 3.3, while deprotonated (anionic) was the main formation at higher pH (>3.3). As to GACs, the interaction with the anionic form was weaker than that with neutral molecule. Then again, pH may also change the functional groups dissociation on GAC surface. Although the FTIR spectra of VRU or WS showed no obvious difference at different pH (see Supporting information, Fig. S13), the increase in pH could change the zeta-potential of both GACs greatly (see Supporting information, Fig. S2). For both GACs, the value of zeta-potential was near 0 mV at pH 3 and enlarged as pH increased. When pH > 9, the zeta-potential of either GAC was more than −40 mV, thus the adsorption capacity of GAC became very weak in strong alkali solution, especially VRU.

4. Conclusions

Two kinds of GACs, VRU and WS proved to be effective for removing bentazon from aqueous solutions, especially VRU. The increasing initial bentazon concentration led to the increase in equilibrium adsorption capacity. The bentazon adsorption process followed the pseudo-second-order model for both VRU and WS, indicating that the adsorption is not just based on rapid-adsorption but on complex processes including intra-particle diffusion and so on. Dubinin–Radushkevich isotherm model best described bentazon adsorption on VRU, while Redlich and Peterson equation fitted the adsorption on WS best, indicating that the adsorption on VRU was a more temperature-dependent process and the intra-particle diffusion played a more important role in the adsorption on WS. The adsorption processes on VRU and WS were all exothermic and mainly belonged to physisorption, although adsorption on VRU including some part of chemisorption. As temperature increased, the adsorption capacities of GACs improved firstly and then fell down, and the inflection point came up nearby 25°C. pH had great influence on the interaction between the pesticides and adsorbents, resulting in decreased GAC adsorption capacity with the increase in solution pH. Even though, the adsorption capacities of both GACs kept stable when initial solution pH was in range 5–9, indicating that both GACs could play an important role in the treatment of actual water in waterworks.

Supplementary material

The supplementary material for this paper is available online at http://dx.doi.10.1080/19443994.2016.1192564.

References

[1] C.O. Ania, F. Béguin, Electrochemical regeneration of activated carbon cloth exhausted with bentazone, Environ. Sci. Technol. 42 (2008) 4500–4506.

[2] A. Derylo-Marczewska, M. Blachnio, A.W. Marczewski, A. Swiatkowski, B. Tarasiuk, Adsorption of selected herbicides from aqueous solutions on activated carbon, J. Therm. Anal. Calorim. 101 (2010) 785–794.

[3] J.M. Salman, M.J. Mohammed, Batch study for herbicide bentazon adsorption onto branches of pomegranates trees activated carbon, Desalin. Water Treat. 51 (2013) 5005–5008.

[4] J.M. Salman, B.H. Hameed, Effect of preparation conditions of oil palm fronds activated carbon on adsorption of bentazon from aqueous solutions, J. Hazard. Mater. 175 (2010) 133–137.

[5] World Health Organization (WHO), WHO Guidelines for Drinking-Water Quality, World Health Organization (WHO), Geneva, 2004.

[6] E.I. Seck, J.M. Doña-Rodríguez, C. Fernández-Rodríguez, O.M. González-Díaz, J. Araña, J. Pérez-Peña., Photocatalytical removal of bentazon using commercial and sol–gel synthesized nanocrystalline TiO$_2$: Operational parameters optimization and toxicity studies, Chem. Eng. J. 203 (2012) 52–62.

[7] R. Otero, D. Esquivel, M.A. Ulibarri, F.J. Romero-Salguero, P. Van Der Voort, J.M. Fernández, Mesoporous phenolic resin and mesoporous carbon for the removal of S-Metolachlor and Bentazon herbicides, Chem. Eng. J. 251 (2014) 92–101.

[8] V.O. Njoku, M.A. Islam, M. Asif, B.H. Hameed, Utilization of sky fruit husk agricultural waste to produce high quality activated carbon for the herbicide bentazon adsorption, Chem. Eng. J. 251 (2014) 183–191.

[9] R. Pourata, A.R. Khataee, S. Aber, N. Daneshvar, Removal of the herbicide Bentazon from contaminated water in the presence of synthesized nanocrystalline TiO$_2$ powders under irradiation of UV-C light, Desalination 249 (2009) 301–307.

[10] D. Mohan, C.U. Pittman Jr., Activated carbons and low cost adsorbents for remediation of tri- and hexavalent chromium from water, J. Hazard. Mater. 137 (2006) 762–811.

[11] K.Y. Foo, B.H. Hameed, Insights into the modeling of adsorption isotherm systems, Chem. Eng. J. 156 (2010) 2–10.

[12] K.Y. Foo, B.H. Hameed, An overview of dye removal via activated carbon adsorption process, Desalin. Water Treat. 19 (2010) 255–274.

[13] E.N. El Qada, S.J. Allen, G.M. Walker, Influence of preparation conditions on the characteristics of activated carbons produced in laboratory and pilot scale systems, Chem. Eng. J. 142 (2008) 1–13.

[14] C. Jung, J. Heo, J. Han, N. Her, S.J. Lee, J. Oh, J. Ryu, Y. Yoon, Hexavalent chromium removal by various adsorbents: Powdered activated carbon, chitosan, and single/multi-walled carbon nanotubes, Sep. Purif. Technol. 106 (2013) 63–71.

[15] J.M. Salman, V.O. Njoku, B.H. Hameed, Bentazon and carbofuran adsorption onto date seed activated carbon: Kinetics and equilibrium, Chem. Eng. J. 173 (2011) 361–368.

[16] C.O. Ania, F. Béguin, Mechanism of adsorption and electrosorption of bentazone on activated carbon cloth in aqueous solutions, Water Res. 41 (2007) 3372–3380.

[17] T. De Wilde, P. Spanoghe, J. Ryckeboer, P. Jaeken, D. Springael, Sorption characteristics of pesticides on matrix substrates used in biopurification systems, Chemosphere 75 (2009) 100–108.

[18] S. Lagergren, Zur theorie der sogenannten adsorption geloester stoffe (About the theory of so-called adsorption of soluble substances), Kungliga Svenska Vetenskapsakad Handlingar 24 (1898) 1–39.

[19] Y.S. Ho, G. McKay, Pseudo-second order model for sorption processes, Process Biochem. 34 (1999) 451–465.

[20] I. Langmuir, The adsorption of gases on plane surfaces of glass, mica and platinum, J. Am. Chem. Soc. 40 (1918) 1361–1403.

[21] H. Freundlich, Über die adsorption in lösungen (Adsorption in solution), Z. Phys. Chem. 57 (1906) 384–470.

[22] O. Redlich, D.L. Peterson, A useful adsorption isotherm, J. Phys. Chem. 63 (1959) 1024–1024.

[23] M.M. Dubinin, L.V. Radushkevich, The equation of the characteristic curve of the activated charcoal, Proc. Acad. Sci. USSR Phys. Chem. Sect. 55 (1947) 331–337.

[24] A. Günay, E. Arslankaya, İ. Tosun, Lead removal from aqueous solution by natural and pretreated clinoptilolite: Adsorption equilibrium and kinetics, J. Hazard. Mater. 146 (2007) 362–371.

[25] A. Dąbrowski, Adsorption—From theory to practice, Adv. Colloid Interface Sci. 93 (2001) 135–224.

[26] K. Vijayaraghavan, T.V.N. Padmesh, K. Palanivelu, M. Velan, Biosorption of nickel(II) ions onto *Sargassum wightii*: Application of two-parameter and three-parameter isotherm models, J. Hazard. Mater. 133 (2006) 304–308.

[27] F. Wang, C.S. Liu, K.M. Shih, Adsorption behavior of perfluorooctanesulfonate (PFOS) and perfluorooctanoate (PFOA) on boehmite, Chemosphere 89 (2012) 1009–1014.

[28] F. Gimbert, N. Morin-Crini, F. Renault, P.M. Badot, G. Crini, Adsorption isotherm models for dye removal by cationized starch-based material in a single component system: Error analysis, J. Hazard. Mater. 157 (2008) 34–46.

[29] P. Chingombe, B. Saha, R.J. Wakeman, Effect of surface modification of an engineered activated carbon on the sorption of 2,4-dichlorophenoxy acetic acid and benazolin from water, J. Colloid Interface Sci. 297 (2006) 434–442.

[30] C.Y. Kuo, C.H. Wu, J.Y. Wu, Adsorption of direct dyes from aqueous solutions by carbon nanotubes: Determination of equilibrium, kinetics and thermodynamics parameters, J. Colloid Interface Sci. 327 (2008) 308–315.

[31] M.J. Jaycock, G.D. Parfitt, Chemistry of Interfaces, Ellis Horwood Ltd., Chichester, 1981.

[32] S.D. Faust, O.M. Aly, Adsorption Processes for Water Treatment, Butterworth, Boston, MA, 1987.